Refining the exchange anisotropy paradigm: Magnetic and microstructural heterogeneity at the Permalloy-CoO interface

A. E. Berkowitz,[1,*] J.-I. Hong,[2] S. K. McCall,[3] E. Shipton,[1] K. T. Chan,[4] T. Leo,[5] and D. J. Smith[5]
[1]*Physics Department, Center for Magnetic Recording Research, University of California–San Diego, La Jolla, California 92093, USA*
[2]*School of Materials Science and Engineering, Georgia Institute of Technology, Atlanta, Georgia 30332, USA*
[3]*Lawrence Livermore National Laboratory, Livermore, California 94550, USA*
[4]*Center for Magnetic Recording Research, University of California–San Diego, La Jolla, California 92093, USA*
[5]*Department of Physics, Arizona State University, Tempe, Arizona 85287-1504, USA*
(Received 4 October 2009; revised manuscript received 24 February 2010; published 5 April 2010)

More than 50 years of extensive research into exchange anisotropy in ferromagnetic-antiferromagnetic bilayers has not produced a convincing explanation for any given system of its principal manifestations, namely, a shift of the hysteresis loop along the field axis (exchange bias) and enhanced coercivity. We have examined this issue in the prototypical polycrystalline Permalloy-CoO bilayer system with samples whose Permalloy thicknesses ranged from 1 to 25 nm. The heterogeneous magnetic and chemical microstructure of the ~1-nm-thick interfacial region is responsible for the observed exchange bias and coercivity, and for their dependence on Permalloy thickness and on temperature. Approximately 75% of the interfacial moment is produced by magnetically hard particles which are exchange coupled to the CoO and are responsible for exchange bias and coercivity by virtue of their exchange coupling to the Permalloy. The remainder of the interfacial moment is produced by a magnetically soft phase that exhibits no exchange bias. The thickness dependence of the exchange bias agrees with the prediction of a random-field model in which the exchange coupling of the distributed hard particles provides a random field operating on the Permalloy. The coercivity is determined by the switching of the hard interfacial particles coupled to the Permalloy; it has a remarkably linear temperature dependence which can be explained by a simple thermal fluctuation model. The exchange bias exhibits the same temperature dependence as the CoO uncompensated spins and these uncompensated spins are on the interfacial {111} planes of the [111]-textured CoO. Finally, the kinetics of the chemical reactions responsible for the interfacial heterogeneity can contribute to the latent period during which the exchange bias can be substantially reversed by applying a field antiparallel to the cooling field.

DOI: 10.1103/PhysRevB.81.134404 PACS number(s): 75.70.Ak, 75.70.Cn, 75.25.−j, 75.60.Jk

I. BACKGROUND

Virtually all current magnetic information storage systems rely on thin-film sensors[1] that utilize the magnetic interaction at the boundary between ferromagnetic (FM) and antiferromagnetic (AFM) thin-film bilayers. This interaction manifests with an enhanced coercive force, H_C, and, more dramatically, as a shift of the hysteresis loop along the field axis. Thus, the loop is not symmetric about $H=0$ but rather offset by an amount called the exchange-bias field (H_{Ex}). Since Meiklejohn and Bean discovered this phenomenon in 1956 and called it exchange anisotropy,[2,3] there has been a strong research effort, well documented in reviews over the past decade,[4–10] to explain the basic mechanisms involved. More specifically, what is the nature of the interfacial exchange interactions in an FM-AFM bilayer that subjects the FM film to a unidirectional anisotropy (H_{Ex}) and increases H_C? Numerous combinations of FM and AFM phases have been investigated to this end and a number of analytical models have been developed to account for the observed behavior.[10] These models have provided plausible descriptions of many examples of the observed behavior in these systems. However, for no bilayer combination has the exchange interaction been modeled to successfully describe the origins of the observed H_{Ex} and H_C, and their dependence on temperature and thickness. A general result of the research on exchange anisotropy has been the recognition that interfacial AFM uncompensated spins (UCS), i.e., spins lacking a compensating antiparallel spin, have a significant role in producing H_{Ex}. However, the origin and role of these UCS has not been reliably established for any bilayer combination.

It is clear that a satisfactory model for the interfacial exchange interaction requires information on the atomic level about the microstructure and chemistry of the interface. This type of information has become more accessible with the impressive improvements in the resolution and element specificity of various x-ray, neutron, and electron techniques. One significant result of these sophisticated investigations is the recognition of the complex nature of the FM-AFM interface and its variation with the phases present, microstructure, degree of epitaxy, preparation conditions, etc. Most of the initial investigations viewed the FM-AFM transition as atomically abrupt and the models were constructed accordingly. While single-crystal bilayers with abrupt interfaces have been prepared by careful molecular-beam evaporation processing, the more usual FM-AFM transition is currently viewed as extending over a number of monolayers with magnetic features varying with the phases present.[10] Polycrystalline bilayers of FM Permalloy (Py) ($Ni_{81}Fe_{19}$) and AFM CoO are frequently used in these investigations; the very low intrinsic H_C of Py makes any H_C enhancement readily apparent while the AFM ordering temperature of CoO ($T_N=291$ K) is convenient for temperature-dependent magnetic measurements. Recent element-specific (Co and Ni) resonant soft

x-ray reflectivity studies[11,12] have provided significant details about the interfacial region between Py and CoO in polycrystalline bilayers. There is an interfacial layer, ~1 nm wide, with composition and magnetic properties that are clearly different from those of Py and CoO. Magnetic Co is present in this interfacial region, together with magnetic Ni and (presumably) Fe. The magnetic Co results from the oxidation/reduction reactions which occur at the interfaces of CoO and NiO with Fe, Co, or Ni.[13] At room temperature, the magnetic Co aligns parallel to the Py and changes direction with the Py as the applied field is reversed. After field cooling from above T_N to 235 K, most of the magnetic Co cycles parallel to the Py in applied fields, with a minor fraction remaining pinned. An investigation of epitaxial single-crystal Py(111)-CoO(111) bilayers employing neutron-diffraction and resonant x-ray scattering has recently confirmed the existence of magnetic Co, both pinned and cycling, at low temperatures and has extensively studied the CoO domain configurations.[14]

The identification of this interfacial layer of finite thickness in Py-CoO bilayers clearly puts a constraint on modeling exchange anisotropy for this system since any FM-AFM exchange is mediated by this region. Furthermore, the x-ray reflectometry results showed how the average Co(Ni) concentration in the interfacial layer diminished (increased) moving away from the CoO to the Py boundary. It seems unlikely, however, that the mixture of Ni-Co-Fe-O in this interfacial layer is homogeneous. Thus, it is essential to determine the microstructure and magnetic properties of the interfacial region in order to formulate a realistic model of exchange anisotropy in this system. This present investigation used a series of polycrystalline Py-CoO bilayers with a range of Py thicknesses. Characterizing the behavior of the magnetically hard and soft phases in the bilayer with 1 nm Py (which replicated the interfacial layer), provided the key to reaching a comprehensive understanding of exchange anisotropy in polycrystalline Py-CoO bilayers as functions of temperature and Py thickness.

II. EXPERIMENTS AND DISCUSSION

The polycrystalline samples prepared for this study were sputtered onto (001) Si wafers with a thin amorphous native oxide surface. The base pressure was $\sim 3 \times 10^{-7}$ Torr. The Py films were sputtered in an Ar atmosphere. The CoO films were reactively sputtered from a Co target in an Ar/O_2 atmosphere. The nominal layer thicknesses were Py(t)/CoO(50 nm), where t was 1, 2, 5, 10, 15, and 25 nm, as indicated by deposition rate calibrations. All films were capped with a 5-nm-thick SiO_2 film to prevent oxidation. Film thicknesses were also measured from cross-sectional transmission electron micrographs of SiO_2(5 nm)/Py(t) films that were deposited on Si wafers simultaneously with the films deposited on CoO, using a substrate support rotating above the sputter guns.

Figure 1(a) is a low-magnification cross-sectional electron micrograph of the SiO_2(5 nm)/Py(10 nm)/CoO(50 nm) sample showing the typical columnar morphology of the CoO layers and the corresponding polycrystalline nature of the Py layers. Figures 1(b)–1(d) are high magnification images for samples with Py thicknesses of 1, 2, and 5 nm, respectively, which emphasize the granularity of the 1 and 2 nm Py layers. The micrographs for thicker films (not shown) show that the Py films generally share the columnar structure of the CoO on which they were deposited, with typical grain diameters of 11–13 nm. For comparison, the enlargements in Fig. 2 show representative cross-sectional areas of the Py films deposited directly onto (001)Si wafers with native oxide. The granular microstructure of the 1 and 2 nm films in Figs. 2(a) and 2(b) precludes determining accurate thicknesses of Py deposited. The TEM thicknesses of the nominal 5, 10, 15, and 25 nm Py films were 5.6 ± 0.3 nm, 10.5 ± 0.3 nm, 17.2 ± 0.4 nm, and 25.7 ± 0.4 nm, respectively. The nominal Py thicknesses are used below when re-

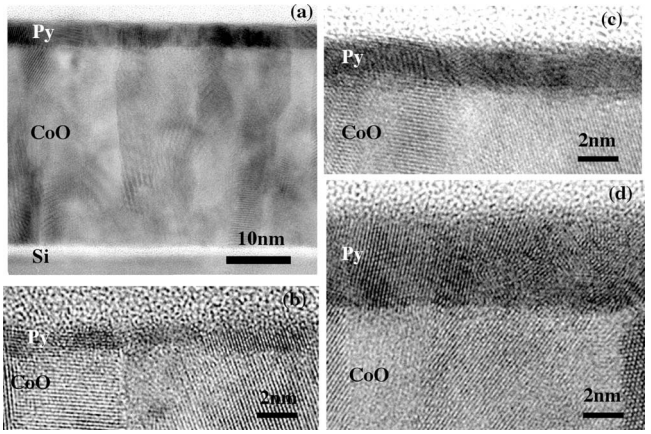

FIG. 1. (a) Low-magnification electron micrograph showing general morphology of Py(5 nm)/CoO(30 nm) bilayer. (b)–(d) High-magnification images of (b) 1 nm Py; (c) 2 nm Py; and (d) 5 nm Py films deposited on 50-nm-thick CoO film.

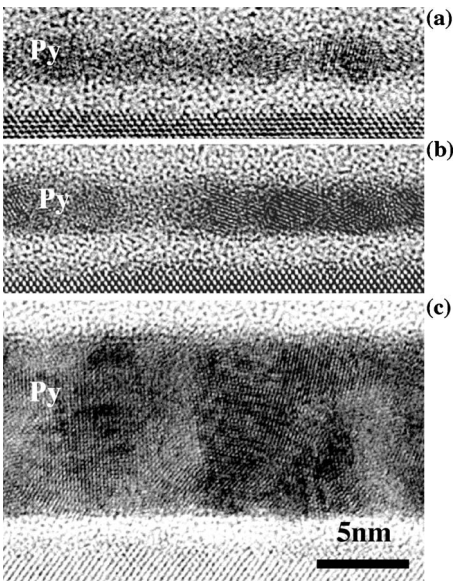

FIG. 2. High-magnification electron micrographs of Py films grown directly on Si(100) substrates with native oxide simultaneously with those on CoO: (a) 1 nm thick; (b) 2 nm thick; and (c) 10 nm thick.

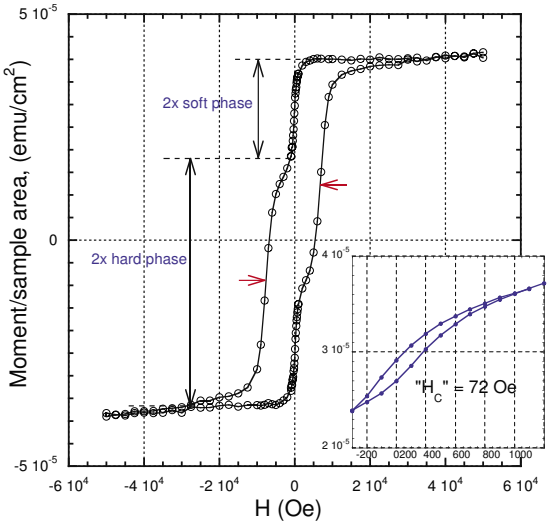

FIG. 3. (Color online) Hysteresis loop of Py(1 nm)-CoO(50 nm) bilayer at 10 K after cooling in 50 kOe from 340 K, with hard and soft phases indicated. Horizontal arrows at midpoints of hard phase, at which fields coercive force, H_C, and exchange-bias field, H_{Ex}, are measured. Inset shows minor loop after several reversals at 300 Oe. H_C taken at widest region of minor loop.

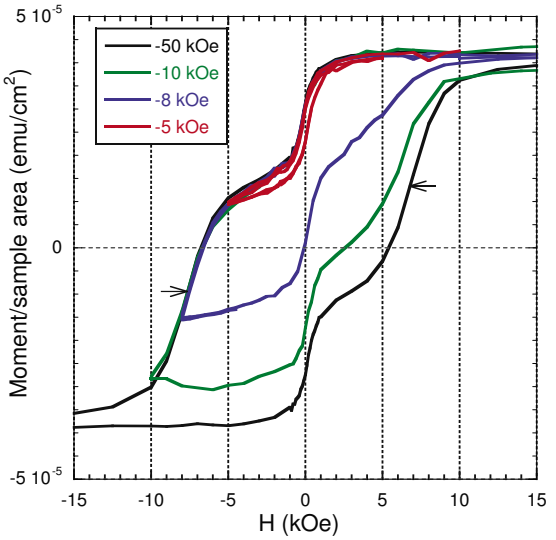

FIG. 4. (Color online) Saturated hysteresis loop (black) with minor hysteresis loops shown superimposed. Saturated hysteresis loop reversed at −50 kOe; minor hysteresis loops reversed at −5, −8, and −10 kOe after +50 kOe saturation. Arrows indicate midpoints of saturated hard phase at which H_{Ex} and H_C are measured.

ferring to the various bilayers; the actual thicknesses measured from the micrographs of Py on Si are used in the data plots.

Figure 3 shows the hysteresis loop of the Py(1 nm) bilayer at 10 K after cooling in 50 kOe from 340 K. Two magnetic phases are clearly distinguished: a soft phase with no significant H_{Ex} and a hard phase with H_C=7315 Oe and H_{Ex} =500 Oe (horizontal arrows indicate the midpoints of the hard phase at which H_C and H_{Ex} were measured). The loop is shifted vertically due to moments pinned in the cooling field direction and the moment of the hard phase is almost three times that of the soft phase. A series of minor loops were measured in order to identify features of the two phases. The inset in Fig. 3 shows the last of several reversals to −300 Oe, used to distinguish the soft phase hysteresis. A nominal H_C=72 Oe was measured at the widest part of the loop, setting an upper limit for the true H_C of the soft phase. Minor loops to −5, −8, and −10 kOe are shown in Fig. 4. They indicate a large region of reversibility. The −5 kOe loop is almost completely reversible. Even the −8 kOe loop produces less than half of the irreversible area in the saturated hysteresis loop. This latter behavior is especially noteworthy since −8 kOe is past the midpoint of the hard phase in the saturated loop, indicated by the arrow, at which H_C and H_{Ex} are defined. The hysteresis loop of the Py(2 nm) bilayer at 10 K also indicated some soft phase, whereas the loops of bilayers with Py$>$2 nm were square, as typified by the loop for Py(10 nm) in Fig. 5.

The properties of the Py(1 nm) bilayer are of major interest since they replicate the properties of the ~1-nm-thick interfacial layer identified by the x-ray reflectivity investigations. A 1 nm magnetic layer is too thin to sustain a domain wall parallel to its plane; therefore the hard and soft phases in Py(1 nm) must consist of neighboring particles. Since the soft particles display negligible H_{Ex}, they are not strongly exchange coupled to the CoO or to the hard particles, with which they share ~1 nm high grain boundaries. The presence of both H_C and H_{Ex} in the hard particles is especially notable. H_C is usually associated with irreversible processes arising from domain-wall pinning or discontinuous magnetization switching, whereas the unidirectional anisotropy that produces H_{Ex} is stable and reversible by definition. Since H_{Ex} in the hard particles arises from exchange coupling with neighboring CoO grains, a reversible rotation of spins in the CoO must occur when the applied field is reversed and the hard particles switch magnetization direction. This spin rotation in the CoO could start at the interface and evolve as a partial domain wall[15] or it could reconfigure existing walls near the interface.

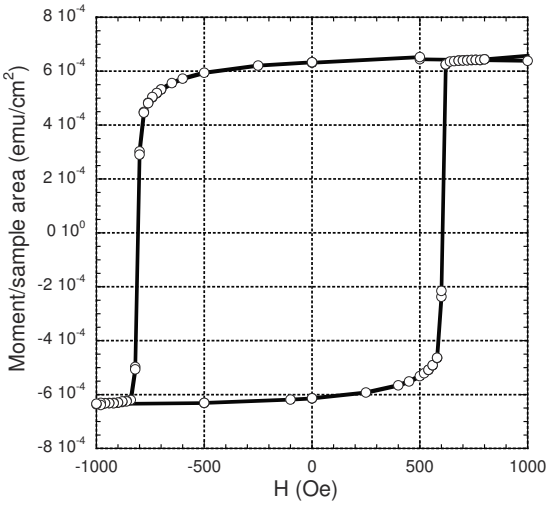

FIG. 5. Hysteresis loop of Py(10 nm)-CoO(50 nm) bilayer at 10 K after cooling in 50 kOe from 340 K.

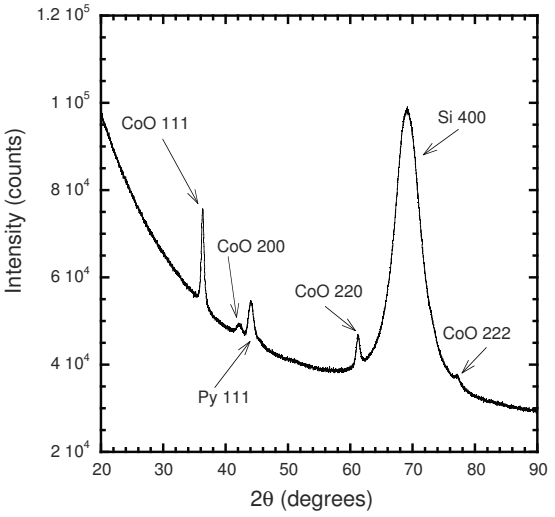

FIG. 6. X-ray diffraction spectra of Py(10 nm)-CoO(50 nm) bilayer. Cu $K\alpha$ radiation. Bragg-Brentano beam geometry.

The interfacial CoO spin configuration is an important issue in these considerations. CoO orders with parallel spins on {111} planes and antiparallel spin directions on alternating {111} planes.[16] Therefore, UCS occupy ideal {111} planes, whereas the spins on all other planes consist of equal numbers of spins in opposite directions, i.e., compensated spins. Thus, after taking roughness into account, [100] and [110] CoO films have predominantly compensated surface spin configurations while [111] CoO films exhibit mostly uncompensated spins on their surfaces. The parallel spin directions on the surfaces of the [111] grains will, of course, vary from one grain to another, i.e., the distribution of the parallel spin directions of the interfacial grains with {111} surfaces will be isotropic about the surface normal. The importance of this feature will be examined below in the discussion of the dependence of H_C on Py thickness. Gökemeijer *et al.*[17] examined epitaxial films of Py on single-crystal films of [100], [110], and [111] CoO, and on [111]-textured CoO. They found no H_{Ex} for Py on [100] and [110], and larger H_{Ex} on the [111]-textured film than on the single-crystal [111] film. We use this strong evidence that H_{Ex} in Py-CoO bilayers appears only with {111} CoO surfaces to explain the behavior of the Py(1 nm)-CoO samples. It is generally recognized that, for energetic reasons, films deposited by sputtering on amorphous substrates such as the native oxide on Si wafers have texture favoring the most densely packed orientation,[18] which is the {111} orientation for CoO. The 50 nm CoO, as well as the Py, in the present bilayers exhibit significant [111] texture in their x-ray diffraction patterns, as shown in Fig. 6 for the Py(10 nm)-CoO(50 nm) bilayer. Since exchange bias requires growth of Py on CoO{111} planes,[17] the presence of [111] CoO texture provides a strong basis for concluding that the hard particles in the Py(1 nm)-CoO(50 nm) bilayer grow on the {111} CoO planes which dominate the Py-CoO interface. Moreover, this exchange configuration and the inverse dependence of [111] texture on CoO thickness serve to clarify the nature of the antiferromagnetic UCS in CoO and their role in exchange bias. Takano *et al.*[19] showed that the temperature dependence of the UCS on the surfaces of polycrystalline CoO films was the same as that of H_{Ex} of Py-CoO bilayers and that H_{Ex} of Py-CoO bilayers increased with decreasing CoO thickness. These features are entirely consistent with a model in which the UCS are the parallel spins on {111} planes of [111]-textured CoO at the Py-CoO interface and their exchange coupling with the hard interfacial particles produces H_{Ex} in these particles. The fact that H_{Ex} decreases with increasing CoO film thickness is a consequence of the decreased [111] texture with increasing CoO thickness.

A very plausible candidate to account for the remarkably high H_C of the hard particles in the Py(1 nm)-CoO(50 nm) bilayer at 10 K is the ferrimagnetic spinel Co-ferrite, $CoFe_2O_4$. At 10 K, the anisotropy field, K_1/M, of $CoFe_2O_4$ is $\approx$40 kOe,[20] quite adequate to produce the observed 7.3 kOe H_C. $CoFe_2O_4$ grows epitaxially on MgO,[21] and CoO and MgO have the same fcc crystal structure, with similar lattice parameters of 4.26 and 4.21 Å, respectively. The spinel Co_3O_4 is the thermodynamically stable oxide of Co at room temperature[22] while CoO is thermodynamically stable above 1200 K and only kinetically stable at room temperature. The growth of the spinel Co_3O_4 on CoO has been reported.[23] Therefore, with the reduction and oxidation reactions that take place in the Py-CoO interfacial layer, it is very reasonable to assume that the hard particles have a spinel structure with composition and anisotropy similar to that of $CoFe_2O_4$. Furthermore, the growth of a spinel structure on {111} planes of the [111]-textured CoO can be described by the modeling of Catlow and Fender[24] to account for Fe_3O_4 clusters in $Fe_{1-x}O$. The usual defect found in transition-metal monoxides such as CoO is a divalent cation vacancy which can be compensated by the formation of trivalent cations. The lowest-energy distributions of the divalent cation vacancies and trivalent cations favor the formation of clusters consisting of four octahedral vacancies surrounding a tetrahedrally coordinated trivalent cation. These clusters energetically tend to aggregate by edge and corner sharing, and one such aggregate is an element of the spinel structure for which bonding on {111} planes is readily accommodated. This was recently demonstrated for the MnO-Mn_3O_4 system in which the ferrimagnetic spinel Mn_3O_4 grows on AFM MnO.[25]

This description of the Py-CoO interfacial $\sim$1-nm-thick layer as consisting of hard particles similar to Co-ferrite, and soft particles, is a new development in exchange anisotropy considerations. The dependence of H_{Ex} and H_C on Py thickness and on temperature are discussed below in terms employing this interfacial microstructure. Therefore it is important to summarize the compelling evidence for this model since we have not been able, as yet, to obtain reliable x-ray diffraction evidence for "cobalt-ferrite-like" particles on the Py(1 nm)-CoO(50 nm) bilayer, where they should be easiest to observe. The difficulty arises from the excessive line broadening due to the $\sim$1 nm thickness and to the additional strain broadening due to epitaxy with the CoO. Nevertheless, the evidence for the existence of hard cobalt-ferrite-like particles in the interfacial layer is very strong. We may summarize this evidence as follows: (a) Figure 3 leaves no doubt of the existence of hard and soft interfacial phases. These phases must be present in the form of hard and soft particles since a planar domain wall cannot exist in the $\sim$1 nm thick-

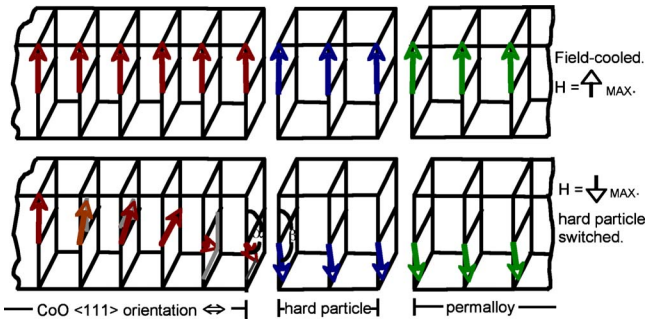

FIG. 7. (Color online) Schematic representation of the {111} spin planes in the interfacial region of the Py-CoO [(green)-(red)] bilayers, with the interfacial layer consisting of a hard particle (blue). For clarity, only half of the CoO spin sublattices ordered on {111} planes are shown. (a) shows the spins of the three phases after field cooling from above T_N(CoO) to a low temperature in a saturating field. In (b), a reverse field at low temperature has irreversibly switched the moment of the hard particle. The exchange coupling of the switched hard particle with the CoO has created a reversible partial domain wall in the CoO, with the resultant angle (β-α) between the spins at the "hard particle"-CoO interface.

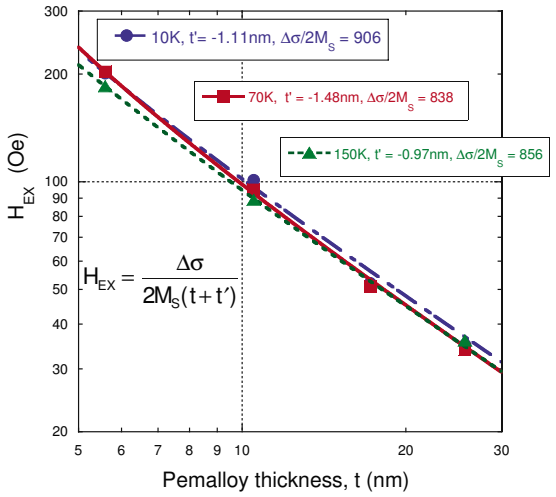

FIG. 8. (Color online) Exchange-bias field, H_{Ex}, vs Py thickness, t, measured at 10, 70, and 150 K after cooling Py(t)-CoO(50 nm) bilayers in 50 kOe from 340 K. Lines through data points show linear fits for $H_{Ex}=\Delta\sigma/2M_S(t+t')$.

ness. (b) The hard particles exhibit both H_C and H_{Ex}. Thus they are exchange coupled to the CoO and H_{Ex} results from the formation of reversible partial domain walls in the CoO as the magnetization in the hard particles is cycled. Figure 7 schematically illustrates these features in a region of the interfacial layer consisting of a hard particle. For clarity, the spins of only one CoO sublattice are shown and the interfaces at which the hard particle is exchange coupled with the CoO and the Py are separated. Figure 7(a) shows the CoO {111} spins in an easy direction induced parallel to the cooling field, by virtue of the interfacial exchange coupling with the hard particle as the bilayer is field cooled through T_N(CoO). In Fig. 7(b), the hard particle has switched at H_C under an applied field. The angle (β-α) between the interfacial exchange-coupled hard particle FM spins and CoO AFM spins identifies an exchange energy, $\sim J_{\text{interface}}\vec{S}_{\text{particle}}\cdot\vec{S}_{\text{CoO}}$, which produces the torque on the hard particle moment that appears as H_{Ex}. The formation of a partial wall in the CoO after the hard particle has switched is depicted in Fig. 7(b). This wall reversibly resumes the spin configuration in Fig. 7(a) as the applied field completes its cycle. There is no contribution to H_C from the reversible partial wall formation in the CoO. H_C results from the irreversible switching of the hard particles' moments in large applied fields. (c) The growth of spinels such as Co-ferrite ($CoFe_2O_4$) on AFM monoxides like CoO is predicted by modeling,[24] confirmed by experiment,[23,25] and is facilitated by the chemical reactions that exist at interfaces between AFM monoxides and 3d FM metals.[13] (d) Finally, as discussed below, all aspects of the dependence of H_{Ex} and H_C on temperature and on Py thickness derive from this model.

Thus the properties of the bilayers with Py>1 nm are mediated by an interfacial region ~ 1 nm thick, consisting of $\sim$75% Co-ferritelike hard particles exchange coupled to both the CoO and the Py, and $\sim$25% soft particles not coupled to the CoO. The hard particles grow on {111} CoO interfacial planes which predominate due to the ⟨111⟩ CoO texture, as depicted in Fig. 7. We now consider the influence of this heterogeneous interfacial layer on the thicker Py films. The most frequently utilized description of the FM-AFM interfacial interaction is Malozemoff's expression for the exchange bias,[26,27]

$$H_{Ex}=\frac{\Delta\sigma}{2M_S t}, \tag{1}$$

where $\Delta\sigma$ is the interfacial FM-AFM coupling energy per unit area, M_S is the FM volume magnetization, and t is the thickness of the FM layer. Since Eq. (1) implicitly assumes a sharp FM-AFM interface with direct FM-AFM exchange coupling, a modification of this expression is expected in order to accommodate the $\sim$1-nm-thick interfacial layer. The dependence of H_{Ex} and H_C on Py thickness and on temperature was measured on bilayers cooled in 25 kOe from 340 K and cycled in 25 kOe ten times to eliminate training effects. In Fig. 8, H_{Ex} at 10, 70, and 150 K is plotted as a function of the TEM Py thickness ($t\geq 5$ nm), showing the fit to $H_{Ex}=\Delta\sigma/2M_S(t+t')$. The fits are excellent for each temperature, with t' on the order of ~ -1 nm in each case, i.e., the true Py thickness must be reduced by ~ 1 nm from the nominal value. This reduction follows directly from the microstructure described above. As noted in the discussion of Fig. 3, H_{Ex} is taken at a reverse field where most of the magnetization of the hard particles has not yet switched, which, in turn, implies that partial walls in the Py are also present. This reduces the effective Py thickness in Eq. (1). The values for $\Delta\sigma/2M_S$ in Fig. 8 are also similar, yielding an average for $\Delta\sigma$ of 0.11 ergs/cm^2, typical of experimental results.[4,8–10]

The magnitude of $\Delta\sigma$ has probably been the subject of most concern since exchange anisotropy was discovered. The nominal problem is that when H_{Ex} is expressed in terms of the basic magnetic parameters, i.e.,

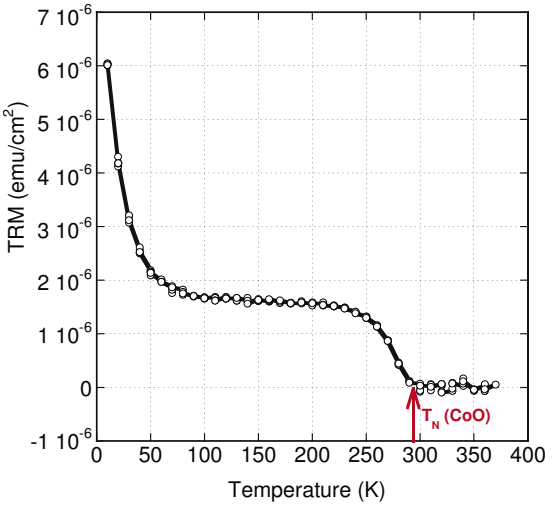

FIG. 9. (Color online) Thermoremanent magnetization of a 20 nm CoO film. Film cooled in 30 kOe from 340 to 5 K and measured in $H=0$.

$$H_{\mathrm{Ex}} = \frac{J_{\mathrm{Ex}}\vec{S}_{\mathrm{FM}} \cdot \vec{S}_{\mathrm{AFM}}}{a^2 M_S t}, \tag{2}$$

where J_{Ex} is the interfacial exchange integral, $\vec{S}_{\mathrm{FM}}$ and $\vec{S}_{\mathrm{AFM}}$ are the spins of the interfacial FM and AFM atoms, respectively, and a is the cubic lattice parameter, the resulting values for $\Delta\sigma = 2J_{\mathrm{Ex}}\vec{S}_{\mathrm{FM}} \cdot \vec{S}_{\mathrm{AFM}}/a^2$ are ≈ 10 ergs/cm^2, i.e., two orders of magnitude larger than observed. This problem vanishes once the role of the interfacial ~ 1 nm layer is recognized. The Py is not directly exchange coupled to the CoO, as most models have assumed. It is exchange coupled to the hard interfacial Co-ferrite-like particles, which, in turn, are exchange coupled to the CoO. As discussed above, any rotation of the magnetization of the hard particles is accompanied by partial wall formation in the CoO; Mauri *et al.*[15] have shown that this reversible process can reduce H_{Ex} by up to several orders of magnitude below that implied by Eq. (2). Furthermore, the soft particles in the interfacial layer do not exhibit any H_{Ex}. In addition, the difference between the lattice spacings of the hard particles and Py will decrease the number of atoms involved in the exchange coupling. Thus, there is no difficulty in accounting for the fact that $\Delta\sigma$ is found to be very much less than calculated from Eq. (2).

There is a general consensus that H_{Ex} involves uncompensated AFM spins. In the present study, the CoO UCS were investigated by measuring the thermoremanent magnetization of a 20 nm CoO film deposited under the same conditions used for the bilayers. Figure 9 shows the temperature dependence of the magnetization of this CoO film after cooling from 340 to 10 K in 25 kOe and measuring the moment in $H=0$ as the sample was warmed. The moment is that of the CoO UCS. The behavior is similar to that previously shown for CoO multilayers,[19] i.e., a sharp "upswing region" below ~ 50 K and a much slower decrease ("plateau region") until ~ 250 K, with a rapid descent to T_N CoO. The temperature dependence of H_{Ex} of the bilayers in the present study, normalized to their values at 10 K, is shown in Fig. 10.

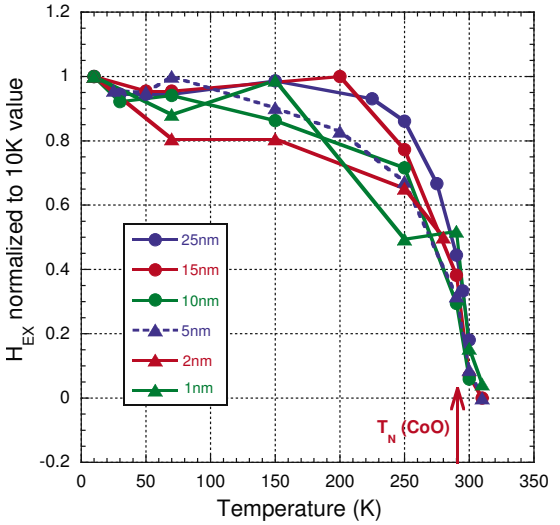

FIG. 10. (Color online) H_{Ex} normalized to values at 10 K of bilayers with indicated Py thicknesses. Samples cooled in 50 kOe from 340 to 10 K and measured at indicated temperatures.

The weak temperature dependence for all samples until ~ 250 K is similar to that of the CoO UCS in Fig. 9 and the very slight increase below ~ 50 K testifies to the different natures of the "plateau" and "upswing" CoO UCS, namely, the UCS in the plateau region are very stiff and do not respond to an applied field, whereas the upswing spins are quite soft, as previously noted.[19] Thus, the temperature dependence of H_{Ex} for these bilayers is quite consistent with the assumption that CoO UCS are involved with the interfacial exchange coupling.

H_C is plotted as a function of Py thicknesses ≥ 5 nm at 10, 70, and 150 K in Fig. 11. For each temperature, the data are fitted to $A(B/t)^X$. The fits are excellent and the fitting exponents are very similar, averaging to 1.52. This is com-

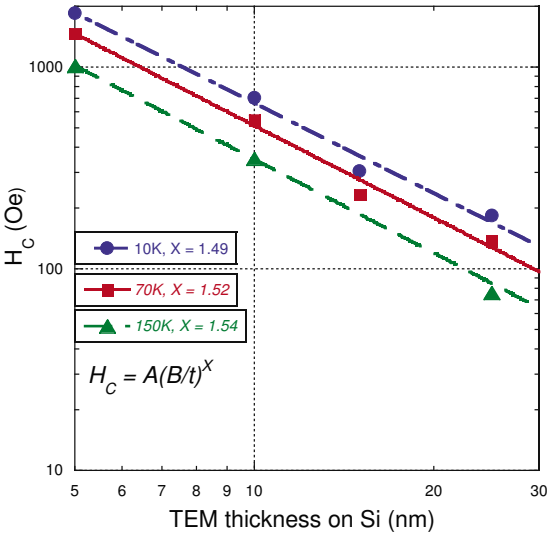

FIG. 11. (Color online) Coercive force, H_C, vs Py thickness, t, at 10, 70, and 150 K after cooling Py(t)-CoO(50 nm) bilayers in 50 kOe from 340 K. Lines through data points show fits to $H_C = A(B/t)^{3/2}$.

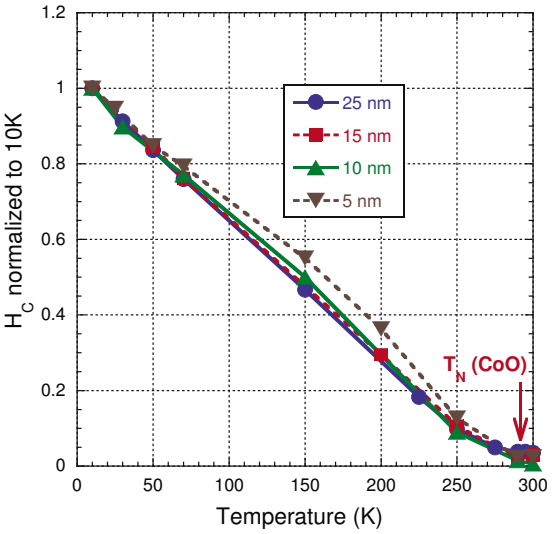

FIG. 12. (Color online) Coercive force, H_C, normalized to 10 K values, vs temperature for Py(t)-CoO(50 nm) bilayers after cooling in 50 kOe from 340 K. Lines through data points are guides to the eye.

parable to the theoretical result of $H_C \propto t^{-3/2}$, obtained by Zhang *et al.*[28,29] from a comprehensive micromagnetic investigation of the behavior of polycrystalline Py-CoO bilayers. Their procedure was to solve the Landau-Lifshitz equation with a Hamiltonian including all magnetic interactions, both internal to, and between, the Py and the CoO films, with isotropically random grains. One basic premise was that the field introduced by considering the interaction between neighboring interfacial FM and AFM sites was randomly determined. Another was the statistical fluctuation of the two AFM sublattices in each AFM grain (finite-size effect). Although it is now evident that direct Py-CoO magnetic interactions do not occur in these bilayers and that the CoO grains are not isotropically oriented, the Py films may still be considered subject to random interactions. The [111] texture of the CoO can accommodate interfacial {111} planes with parallel spin directions isotropically distributed around the normal to the surface. Furthermore, the interfacial chemical reactions responsible for the Co-ferritelike structure of the hard particles can include reactions with CoO {111} planes tilted somewhat from the interfacial plane. These factors will randomize the easy directions of the hard particles to which the Py is exchange coupled, thereby providing an effective random field on the Py. This description of the origin of the random fields is considerably more transparent than deriving the behavior of the Py from random interactions between spins on neighboring Py-CoO atomic sites. Thus the exchange coupling of Py with hard interfacial Co-ferrite-like particles is the major factor in determining H_C of the Py films since this interaction provides the random field in the elegant analysis of Zhang *et al.*[28,29]

More direct insight into the role of the hard particles in determining H_C is derived from its temperature dependence. In Fig. 12, the temperature dependence is shown for the thicker films for values normalized to 10 K. The linear behavior for all four films up to ~250 K is quite evident and strongly suggests thermal activation. A simple explanation follows from considering the manner in which the hard particles pin the Py films to which they are exchange coupled. As the domain walls are driven past the underlying hard particles, narrow partial walls form in the Py above them. The hard particles are now subject to thermal fluctuation fields that can assist in switching them. The concept of thermal fluctuation fields arises from the observation that the magnetization of relatively hard materials in fixed reverse fields generally declines logarithmically over time, a phenomenon termed "magnetic viscosity." Consideration of the activation energy, E, responsible for this behavior led to an expression for an effective thermal fluctuation field operating on these materials,[30]

$$H_f = \frac{-kT}{dE/dH}. \tag{3}$$

Another form, more convenient for the present purpose, is[31]

$$H_f = \frac{kT}{VM_S}, \tag{4}$$

where V is the volume switched as a domain wall jumps from one pinning center to another and M_S is the spontaneous magnetization involved. The volume is essentially that of the hard particles and Eq. (4) expresses the energy reduction produced by the thermally activated switching of these particles' magnetizations into the field direction. The temperature dependent H_C of these particles now becomes

$$H_C(T) = [H_{Ci}(T) - H_f(T)], \tag{5}$$

where $H_{Ci}(T)$ is the intrinsic H_C of the hard particles in the absence of thermal fluctuations. The linear region in Fig. 12 extends to 250 K, the termination of the plateau region for the UCS, as shown in Fig. 9. H_f(250 K) is estimated by taking $V=(10\times10\times1)$ nm^3 for the volume of the hard particles and $M_S=500$ Oe (for $CoFe_2O_4$) in Eq. (4). This gives H_f(250 K) $\approx$700 Oe. Such a value for H_f(250 K) indicates that $H_f(T)$ is quite adequate to produce a closely linear temperature dependence for H_C as $H_f(T)$ increases linearly with T. Several factors contribute to the virtual vanishing of H_C near T_N (CoO). It is generally accepted that for superconducting quantum interference device measurements which require about 1 min per point, the expression K_pV/kT, where K_p is the anisotropy constant of a particle with volume V, should be ~25 for magnetic thermal stability. However, $K_pV/kT\approx8$ at T_N(CoO) for the hard particles, using the estimated V above and $K_p(CoFe_2O_4)$ (Ref. 20) at 300 K, which indicates the onset of superparamagnetic relaxation with $H_C\approx0$. Furthermore, inasmuch as the hard particles are exchange coupled to the CoO at their interface, it is likely that they benefit from a proximity effect which would stabilize them further against superparamagnetic relaxation. This proximity effect disappears when the CoO becomes paramagnetic.

The microstructural and magnetic heterogeneity in the Py-CoO interfacial layer provides the basis for explaining another aspect of exchange anisotropy. It is generally recognized that H_{Ex} can be established in an FM-AFM bilayer by two quite different protocols: (a) cooling the bilayer from

above T_N(AFM) in a field sufficient to saturate the FM or (b) depositing the FM below T_N(AFM) in an applied field. These two protocols were specifically shown to yield equivalent behavior for bilayers of Co-($Ni_{0.52}Co_{0.48}O$).[32] Application of these protocols to Py/CoO bilayers can be considered as follows. In (a), above T_N, the FM film is polarized but the hard interfacial Co-ferritelike particles are paramagnetic since they incorporate ordered CoO {111} planes of parallel spins which are paramagnetic. As the temperature is reduced below T_N, the exchange coupling with the polarized Py induces the hard particles to order with easy directions closest to the cooling field direction. This requires that the {111} CoO planes of parallel spins incorporated in the hard Co-ferritelike particles select their most accommodating easy directions. In (b), the interfacial chemical reactions that produce the Co-ferritelike particles take place under a polarizing magnetic field which induces easy directions closest to the field direction. The directions of the parallel spins in the incorporated CoO {111} planes in these particles are again those most accommodating to the easy directions of the respective hard particles. The explanations for both of these protocols might seem to suggest that an applied field high enough to switch the hard particles should be able to reorient the net easy direction of the CoO-hard particle-Py assembly while the unidirectional axis was being established. In fact the Co-($Ni_{0.52}Co_{0.48}O$) bilayer study showed that, indeed, there was a "latent period" of something more than 20 min (and less than two months) after deposition of the Co on the ($Ni_{0.52}Co_{0.48}O$) below T_N during which the biasing direction could be substantially, but not completely, reversed.[32] This latent period could reflect the kinetics of the oxygen and vacancy diffusion involved with the chemical reactions[13] that produce the heterogeneous interfacial layer. A final stable biased state is reached when the magnetoelastic energies arising from the localized spin states reach a global minimum consistent with the ambient temperature and the respective spin states become "locked in."

III. SUMMARY

The basis for this investigation of polycrystalline Py-CoO bilayers was the resonant x-ray reflectivity demonstration that an interfacial layer ~1 nm thick existed in this system, with properties that were different from either Py or CoO. The present study has produced significant new insights into the nature of exchange anisotropy in this prototypical system. It has shown that the interfacial layer consists of ~75% hard particles exchange coupled to the CoO and ~25% soft particles that are not exchange coupled. Consideration of composition, structure, and properties issues involving these hard particles plausibly suggests that they are similar to $CoFe_2O_4$. The hard particles exhibit both H_{Ex} and H_C,. This combination of properties is facilitated by the reversible formation of partial domain walls in the CoO as the hard particles switch their magnetizations. Thus, direct exchange between Py and CoO does not occur; it is mediated by hard particles that are exchange coupled to the CoO.

Defining the microstructural origins of the magnetic properties of the heterogeneous interfacial layer in Py-CoO has served to clarify several exchange anisotropy puzzles in this system, as well as explaining the temperature and Py thickness dependence of H_C and H_{Ex}. The magnitude of $\Delta\sigma$ is strongly reduced from its upper limit mainly by the creation of partial domain walls in the CoO, to a lesser extent by atomic mismatch at the Py-spinel interface, and by the presence of some interfacial regions with no exchange coupling. The Py thickness (t) in the "$1/t$ law" for H_{Ex} is reduced from its nominal value principally by the strong reversible region in the hysteresis loop which is due to the fact that the hard particles do not switch until fields larger than the apparent H_C are applied. The uncompensated spins which participate in establishing H_{Ex} are on {111} planes of the [111]-textured CoO and thus the temperature dependence of H_{Ex} follows that of the UCS. The distributed nature of the hard interfacial particles constitutes a random field for the Py film to which they are exchange coupled, thereby yielding a "$t^{-3/2}$" dependence for H_C, as predicted for interfacial random fields. The surprisingly linear dependence of H_C on temperature for Py thicknesses ≥ 5 nm is a straightforward example of the operation of thermal fluctuation fields. Finally, the two protocols for establishing H_{Ex} are explained by the development of the microstructural chemistry and consequent magnetic properties of the interfacial region, as is the latent period during which H_{Ex} can be substantially reversed by an applied field.

The question remains as to whether these results on polycrystalline samples hold for single crystals. The recent paper by Radu *et al.*[14] indicates similar behavior. That paper reports on an epitaxial (111) Py(12 nm)-CoO(500 nm) bilayer. H_{Ex} had the same temperature dependence as for the Py(10 nm) sample in Fig. 10, with $H_{Ex}(10\ \mathrm{K})$ ~25% of the value indicated in Fig. 8. A lower H_{Ex} might be expected due to lesser constraints on partial walls in a thick single-crystal CoO as compared to a thinner CoO grain with an 11–13 nm diameter. The H_C values were essentially the same as those derived for Py(12 nm) from Fig. 11. A linear temperature dependence was also reported, similar to that in Fig. 12. These results would suggest that an interfacial layer is present in the single-crystal sample, comparable to the one in the polycrystalline bilayer.

These findings constitute the most complete description of the manifestations of exchange anisotropy in a given system. Are they relevant to the wide range of FM-AFM systems of technological and scientific interest? While it is certain that the chemistry and microstructure of the interface will vary with the FM and AFM phases present, it is also likely that an interfacial phase is present with properties different from either of the parent phases. This seems to be the case even for nonionic AFM phases, as indicated in a recent study of the MnPd-Fe system.[33] Therefore, a significant general result is that the key to explicating the heterogeneous microstructural and magnetic nature of the interfacial layer in the Py-CoO system was the examination of the properties of the bilayer with 1 nm Py, which replicated the interfacial layer. A similar experiment in any bilayer system should prove equally useful.

ACKNOWLEDGMENTS

We appreciate useful discussions with F. E. Spada and E.

E. Fullerton. Work performed at LLNL was under the auspices of the U.S. Department of Energy by Lawrence Livermore National Laboratory under Contract No. DE-AC52-07NA2734. We acknowledge the use of facilities at the John M. Cowley Center for High Resolution Electron Microscopy at Arizona State University.

*aberk@ucsd.edu

[1] J. C. S. Kools, IEEE Trans. Magn. **32**, 3165 (1996).
[2] W. H. Meiklejohn and C. P. Bean, Phys. Rev. **102**, 1413 (1956).
[3] W. H. Meiklejohn and C. P. Bean, Phys. Rev. **105**, 904 (1957).
[4] J. Nogués and I. K. Schuller, J. Magn. Magn. Mater. **192**, 203 (1999).
[5] A. E. Berkowitz and K. Takano, J. Magn. Magn. Mater. **200**, 552 (1999).
[6] R. L. Stamps, J. Phys. D **33**, R247 (2000).
[7] M. Kiwi, J. Magn. Magn. Mater. **234**, 584 (2001).
[8] J. Nogués, J. Sort, V. Langlais, V. Skumryev, S. Suriñach, J. S. Muñoz, and M. D. Baro, Phys. Rep. **422**, 65 (2005).
[9] A. E. Berkowitz and R. H. Kodama, *Nanomagnetism 1; Multilayers, Ultrathin Films, and Textured Media*, edited by J. A. C. Bland and D. L. Mills (Elsevier, Amsterdam, 2006), Chap. 5.
[10] F. Radu and H. Zabel, Springer Tracts Mod. Phys. **227**, 97 (2008).
[11] S. Roy, C. Sanchez-Hanke, S. Park, M. R. Fitzsimmons, Y. J. Tang, J. I. Hong, David J. Smith, B. J. Taylor, X. Liu, M. B. Maple, A. E. Berkowitz, C.-C. Kao, and S. K. Sinha, Phys. Rev. B **75**, 014442 (2007).
[12] E. Blackburn, C. Sanchez-Hanke, S. Roy, D. J. Smith, J.-I. Hong, K. T. Chan, A. E. Berkowitz, and S. K. Sinha, Phys. Rev. B **78**, 180408(R) (2008).
[13] T. J. Regan, H. Ohldag, C. Stamm, F. Nolting, J. Lüning, and J. Stöhr, Phys. Rev. B **64**, 214422 (2001).
[14] F. Radu, S. K. Mishra, I. Zizak, A. I. Erko, H. A. Dürr, E. Eberhardt, G. Nowak, S. Buschhorn, H. Zabel, K. Zhernekov, M. Wolff, D. Schmitz, E. Schierle, E. Dudzik, and R. Feyerherm, Phys. Rev. B **79**, 184425 (2009).
[15] D. Mauri, H. C. Siegmann, P. S. Bagus, and E. Kay, J. Appl. Phys. **62**, 3047 (1987).
[16] W. L. Roth, Phys. Rev. **110**, 1333 (1958).
[17] N. J. Gökemeijer, R. L. Penn, D. R. Veblen, and C. L. Chien, Phys. Rev. B **63**, 174422 (2001).
[18] L. Dong and D. J. Srolovitz, J. Appl. Phys. **84**, 5261 (1998).
[19] K. Takano, R. H. Kodama, A. E. Berkowitz, W. Cao, and G. Thomas, Phys. Rev. Lett. **79**, 1130 (1997).
[20] H. Shenker, Phys. Rev. **107**, 1246 (1957).
[21] A. Lisfi, C. M. Williams, L. T. Nguyen, J. C. Lodder, A. Coleman, H. Corcoran, A. Johnson, P. Chang, A. Kumar, and W. Morgan, Phys. Rev. B **76**, 054405 (2007).
[22] N. N. Greenwood and A. Earnshaw, *Chemistry of the Elements* (Butterworth-Heinemann, Amsterdam, 1997), p. 1113.
[23] Y. Wang, Y. Zhang, Y. Cao, and M. Y. Lu, J. Alloys Compd. **450**, 128 (2008).
[24] C. R. A. Catlow and B. E. F. Fender, J. Phys. C **8**, 3267 (1975).
[25] A. E. Berkowitz, G. F. Rodriguez, J. I. Hong, K. An, T. Hyeon, N. Agarwal, D. J. Smith, and E. E. Fullerton, J. Phys. D **41**, 134007 (2008).
[26] A. P. Malozemoff, Phys. Rev. B **35**, 3679 (1987).
[27] A. P. Malozemoff, J. Appl. Phys. **63**, 3874 (1988).
[28] S. Zhang, D. V. Dimitrov, G. C. Hadjipanayis, J. W. Cai, and C. L. Chien, J. Magn. Magn. Mater. **198-199**, 468 (1999).
[29] Z. Li and S. Zhang, Phys. Rev. B **61**, R14897 (2000).
[30] D. H. L. Ng, C. C. H. Lo, and P. Gaunt, IEEE Trans. Magn. **30**, 4854 (1994), and references therein.
[31] E. P. Wohlfarth, J. Phys. F: Met. Phys. **14**, L155 (1984).
[32] A. E. Berkowitz, M. F. Hansen, R. H. Kodama, Y. J. Tang, J. I. Hong, and D. J. Smith, Phys. Rev. B **72**, 134428 (2005).
[33] S. Brück, G. Schütz, E. Goering, X. Ji, and K. Krishnan, Phys. Rev. Lett. **101**, 126402 (2008).